Rakenteiden Mekaniikka (Journal of Structural Mechanics)
Vol. 58, No. 2, 2025, pp. 33–45
https://rakenteidenmekaniikka.journal.fi/index
https://doi.org/10.23998/rm.152288
© 2025 The Authors
Open access under the license CC BY 4.0

VERTAISARVIOITU
KOLLEGIALT GRANSKAD
PEER-REVIEWED
www.tsv.fi/tunnus

Design of a non-linear wire-rope tuned mass damper – linearized model-based approach

Samuli Rytömaa[1], Sampo Laine and Raine Viitala

Summary Wire rope springs are used in tuned mass damper applications due to their inherent energy dissipation properties, low cost, thermal stability and mechanical robustness. The dynamics of the wire rope springs are characterized by the relative sliding of the strands inside the wire ropes. Damping of the wire rope consists of the friction loss between the wire strands and structural damping under mechanical deformations. Moreover, the relative sliding alters the effective stiffness of the structure. These properties are non-linear and depend on the vibration amplitude. Modeling these non-linear dynamics has proven difficult, and no clear standard approach for design exist. In this paper, an amplitude based linearization framework is used to model the system dynamics for wire rope based tuned mass damper. The vibration suppression performance of the wire-rope tuned mass damper is compared to a linear tuned mass damper with similar mass ratio. The performance of the two dampers are compared for a system with multiple degrees of freedom, and the possible mistuning of the dampers is also considered. The results show that wire rope based tune mass damper, in comparison to a conventional linear tuned-mass damper, can suppress vibrations with a wider frequency band and under varying natural frequencies.

Keywords: structural dynamics, tuned mass damper, wire rope spring

Received: 28 November 2024. Accepted: 11 March 2025. Published online: 23 June 2025.

Introduction

Excessive vibrations are a common cause for industrial machinery failures and productivity losses. The most severe of these vibration conditions is resonance, which in some cases cannot be avoided. While previously machinery have often had a constant operational speed, modern machines have multiple operational speeds due to the increased use of variable frequency drives. The wider operational speed range can excite multiple resonance frequencies, which has created a need for wider band vibration mitigation methods. Additionally, applications experiencing varying natural frequencies can benefit from tuned mass dampers robustness to this variation.

Tuned mass dampers (TMD) have been used to solve resonance problems for over a hundred years since their first invention [6, 9]. The TMD is an auxiliary mass attached to the vibrating structure using springs. The mass and stiffness of this auxiliary element are tuned so that its tuning frequency is the same as of the vibrating structure. The damper

[1]Corresponding author: samuli.rytomaa@aalto.fi

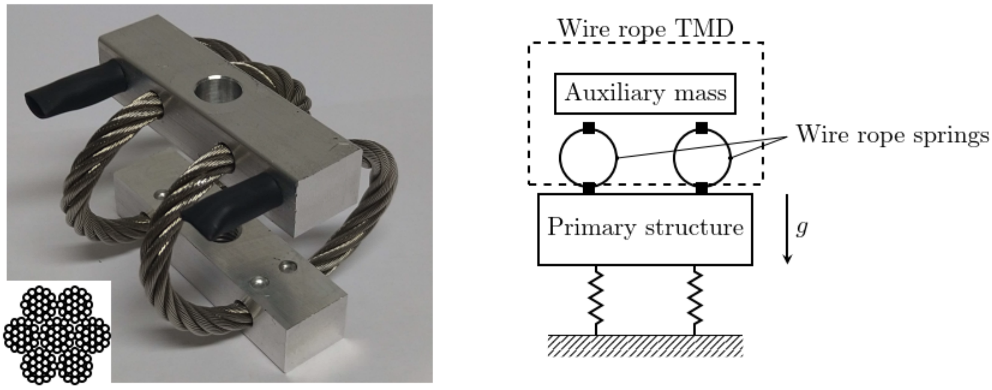

a) b)

Figure 1. On the left (a) is a wire rope spring, made from metal pieces that are connected to each other using steel wire rope. The loop diameter of this wire rope spring is 32 mm and the wire diameter is 5 mm. The wire rope cross section is presented in the lower left corner. On the right (b) is an example arrangement of wire rope tuned mass damper used in this study. The auxiliary mass is placed on top of wire rope springs, which creates a compressive preload on the springs.

will create a counteracting force to eliminate the vibration of the primary structure. The tuned mass damper works only on a small frequency band, and its effective range can be extended by adding a damper in series with the spring. Optimal design parameters have been proposed in [9, 2]. Even with the damper element attached, the resulting frequency band is still quite limited. Regardless of the limitations, tuned mass dampers are a widely used solution for vibration problems.

Nonlinear tuned mass dampers have recently attracted research interest due to their larger operational frequency band. Initially the research has focused on nonlinear stiffness [1, 29, 17], but has since moved to nonlinear damping [25, 28, 24] and their combined use [10]. Most of the research has been purely mathematical, where the source of nonlinearity has not been specified. Several studies have proposed using shape memory materials[21] and magneto-rheological fluids [16, 20] to achieve the nonlinearity. Researchers have proposed nonlinear tuned mass dampers based on other phenomena, such as friction [11, 23], fluid sloshing [5] and particle collisions [19, 18]. One method of incorporating nonlinear stiffness and damping has been the use of wire rope springs.

Wire rope springs (WRS), (often also called wire rope isolators) have seen increased research in the past years due to their nonlinear hysteretic behavior. The wire rope spring is created by connecting two metal pieces together using steel wire rope, as shown in Figure 1 a). There are endless possibilities for the design, such as wire rope diameter, loop sizes and number of loops. Under dynamic loading, the strands inside the wire ropes start to slide relative to each other, which dissipates energy and changes the stiffness [30, 22, 13]. The relationship between the stiffness and damping to the vibration amplitude is nonlinear [30], making the WRS a promising component for nonlinear tuned mass damper. The hysteresis loop is unsymmetric, when the loading alternates between tension and compression [4]. Previous research has proposed a TMD based on a straight wire rope [3, 12], as well as a pendulum type TMD with wire rope spring [7, 8]. No research has been proposed for a tuned mass damper, where the auxiliary mass is placed on top of the WRSs as shown in Figure 1 b). However, there exists a patented solution [15]. Wire rope spring based solutions are especially useful for applications where oil is not allowed or when high temperature variations are expected.

This paper presents a study on the dynamics of a wire rope tuned mass damper based on wire rope springs, which has not been previously considered in the literature. Linearized model for the wire rope spring proposed in [27] is used to simulate the steady state response of two different systems. The calculated response is compared to undamped system and system with a linear tuned mass damper of equal mass ratio. The results show that nonlinear TMD can be advantageous when wider frequency band for damping is required.

Methods

The wire rope tuned mass damper (WRTMD) in this study consists of an auxiliary mass, placed on top of the wire rope springs as shown in Figure 1 b). The wire rope springs are then attached onto the structure with problematic resonance. The auxiliary mass should keep the wire rope springs under compression during normal operation. The following section presents the modeling method for the wire rope springs, and the description of the modeled systems.

Wire rope spring model

The steady state dynamics of the wire rope spring are modeled according to the method proposed in [27]. This model uses an amplitude based linearization for the effective amplitude dependent stiffness and damping. The damping is modeled as complex stiffness, which captures the rate independent damping phenomena under steady state conditions. The model applies only for small displacements, where the hysteresis loop is on the compressive side. With higher loads, a more sophisticated model accounting for the asymmetric shape would be required. The mathematical model showed good agreement with measurements for a base excitation type problem. This section details the mathematical model used in this study.

To use the amplitude based linearization method, the effective stiffness and damping values were identified from experiments. An amplitude controlled shaker test was used to measure the hysteresis loops of the WRSs with different amplitudes for a certain preload level. The preload was applied as mass placed on top of the wire rope springs. The excitation frequency was kept below the natural frequency of the testing setup. An example hysteresis loop at three different amplitudes is given in Figure 2 a). The nonlinearity in hysteresis loops is due to two sources, which both arise from the wire rope internal friction. Firstly, the cross-section of the wire is stiffer when the strands stick to each other behaving almost as it was solid. Secondly, the friction dissipates energy. From the hysteresis loops, the effective stiffness and loss energies were identified for each vibration amplitude. These two quantities can be used to calculate the effective damping for the WRS.

The effective stiffness k_{eff} of the WRS is obtained from the ends of the hysteresis loops. A third order polynomial was fitted to the measured effective stiffness data, given below:

$$k_{\text{eff}}(x_a) = ax_a^3 + bx_a^2 + cx_a + d \tag{1}$$

where x_a is the vibration amplitude of the wire rope spring and a, b, c and d are the fitted polynomial coefficients. The resulting curve used in this study is presented in Figure 3. The Figure shows that the effective stiffness decreases as the vibration amplitude increases. The wire rope spring vibration amplitude x_a is defined as the amplitude of vibration between the degrees of freedom that are attached to the wire rope spring.

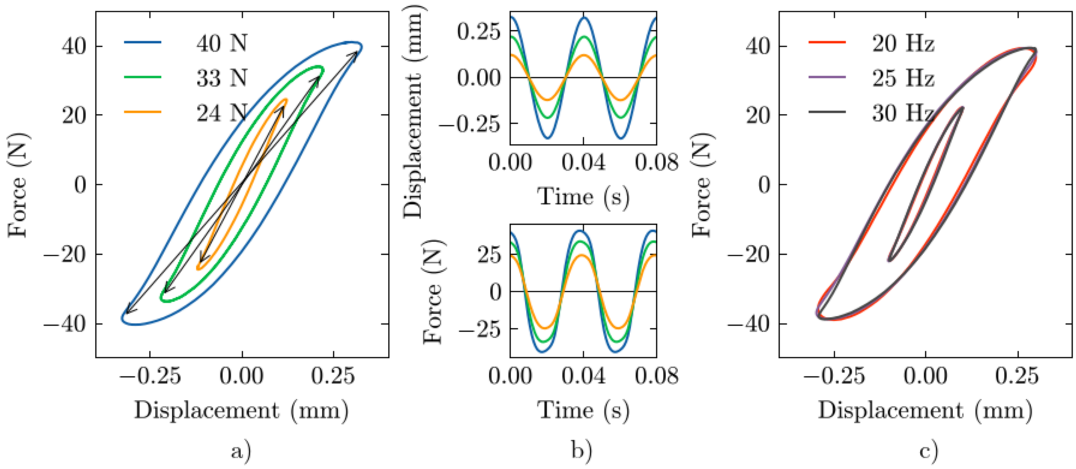

Figure 2. Example hysteresis loop with multiple excitation amplitudes (a) and various excitation frequencies (c), from [27].The middle figures (b) show the time signals used to create the hysteresis loops in a). The preload for a single wire rope spring is 80 N, meaning that the loops are completely on the compressive side. The model parameters for the WRS dynamic model are obtained from these loops. The effective stiffness is obtained from the maximum and minimum amplitudes (arrows in a), while the loss energy is obtained from the area of the hysteresis loop. The figure a) shows that the effective stiffness of the WRS decreases as the amplitude of vibration increases and that the response does not depend on loading frequency. The plot in c) shows that the behavior does not depend on the excitation frequency.

Loss energy was obtained from the area of the hysteresis loops. The loss energy gives the energy dissipated by the WRS during a single oscillation cycle. A piece-wise function was fitted to the measured loss energy data, shown in the following equation

$$W_{\text{loss}}(x_a) = \begin{cases} a_1 x_a^2 + b_1 x_a + c_1, & x_a < x_{\text{threshold}} \\ b_2 x_a + c_2, & x_a \geq x_{\text{threshold}} \end{cases}, \; W_{\text{loss}} \geq 0 \tag{2}$$

where x_a is the vibration amplitude, a_1, b_1, c_1, b_2 and c_2 are coefficients for the polynomials and $x_{threshold}$ is a threshold amplitude where the polynomial function changes. The assumption for this model is, that with very small amplitudes, material damping dominates the energy loss, which is described with the second order term. The linear term represents Coulomb friction. At some amplitude $x_{threshold}$, the Coulomb friction becomes the dominant phenomena, and the square term vanishes. Since both linear and square terms of the polynomial are based on physical energy loss phenomena, the values of the coefficients must be positive, otherwise the terms would not contribute to energy dissipation. The values for the parameters are found by fitting the energy loss equation to the measured data. The resulting energy loss plot is shown in Figure 3.

The amplitude dependent loss factor is defined as the ratio between dissipated energy and the elastic energy of the spring. The equation for the loss factor is

$$\eta(x_a) = \frac{W_{\text{loss}}(x_a)}{2k_{\text{eff}}(x_a)x_a^2} \tag{3}$$

where k_{eff} is the effective stiffness of the WRS at given amplitude. The resulting graph for the loss factor is shown in Figure 3. This loss factor can be directly used for the complex stiffness term. The resulting equation of motion for the one degree of freedom wire rope tuned mass damper is

$$m\ddot{x} + k_{\text{eff}}(x_a)(1 + i\eta(x_a))x = f(t) \tag{4}$$

where m is the auxiliary mass used in the tuned mass damper, i is the imaginary unit and $f(t)$ is the excitation force. As per the steady-state assumption, the response $x(t)$ is defined as

$$x(t) = x_a e^{i(\omega t+\phi)} \tag{5}$$

where ω is the frequency of the excitation, and ϕ is the phase. The equation of motion can be directly inserted into the set of equation representing the whole vibrating system.

As the equation of motion for the WRS is nonlinear due to the response amplitude dependent stiffness and damping terms, the solution requires iteration. The iteration is scheme is given below:

1. Assume initial vibration amplitude for the wire rope spring x_a, such as 0.1 mm or previous solution.
2. Calculate the values for k_{eff} and η using the previous x_a.
3. Solve system response, and obtain new vibration amplitude x_a for the wire rope spring from the calculated response.
4. Repeat until vibration amplitude converges. In this study the convergence value was set to 1 µm.
5. If final amplitude is outside of the identification range, print a warning.

The equations of motion for a larger system with wire rope tuned mass damper is

$$\mathbf{M}\ddot{\mathbf{x}}(t) + \mathbf{C}\dot{\mathbf{x}}(t) + \mathbf{K}(\mathbf{x})\mathbf{x}(t) = \mathbf{f}(t) \tag{6}$$

where $\mathbf{M}$, $\mathbf{C}$ and $\mathbf{K}$ are the mass, damping and stiffness matrices, and $\mathbf{x}$ and $\mathbf{f}$ are the displacement and force vectors. The stiffness matrix is nonlinear as it depends on the displacement vector. For the case of 2 degree of freedom model (Figure 4 a)), the equation of motion is

$$\begin{bmatrix} m_1 & 0 \\ 0 & m_2 \end{bmatrix} \ddot{\mathbf{x}} + \begin{bmatrix} c_1 & 0 \\ 0 & 0 \end{bmatrix} \dot{\mathbf{x}} + \begin{bmatrix} k_1 + k(x_a)(1+i\eta(x_a)) & -k(x_a)(1+i\eta(x_a)) \\ -k(x_a)(1+i\eta(x_a)) & k(x_a)(1+i\eta(x_a)) \end{bmatrix} \mathbf{x} = \begin{bmatrix} f_1 \\ 0 \end{bmatrix} \tag{7}$$

$$\mathbf{x} = \begin{bmatrix} x_1 e^{i\phi_1} \\ x_2 e^{i\phi_2} \end{bmatrix} e^{\omega t}, \mathbf{f} = \begin{bmatrix} f_1 \\ 0 \end{bmatrix} e^{i\omega t} \tag{8}$$

where x_j is the displacement amplitude, f_j is the force magnitude, ϕ_j is the phase of mass j and ω is the frequency of the response and forcing. The vibration amplitude x_a is calculated directly from the system response. In this case the amplitude of the wire rope spring is

$$x_a = |x_1 e^{i\phi_1} - x_2 e^{i\phi_2}| \tag{9}$$

The tuning frequency of the wire rope tuned mass damper depends on the amplitude of vibration. This means that it can tune in to multiple resonance frequencies. The tuning frequency is calculated with

$$w_{\text{tuning}}(x_a) = w_n(x_a)\sqrt{1-\xi(x_a)^2} = \sqrt{\frac{k_{\text{eff}}(x_a)}{m}}\sqrt{1-(\eta(x_a)/2)^2} \tag{10}$$

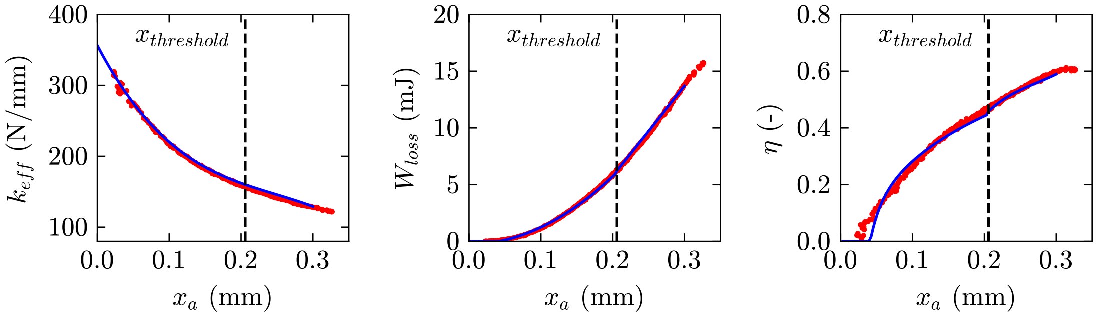

Figure 3. The amplitude dependent stiffness k_{eff}, loss energy W_{loss} and loss factor η of the wire rope spring as a function of vibration amplitude x_a. The small discontinuity comes results from the loss energy model changing mechanism at the threshold amplitude $x_{\text{threshold}}$. The red dots are the measured values used to fit the parameters of the mathemtaical model.

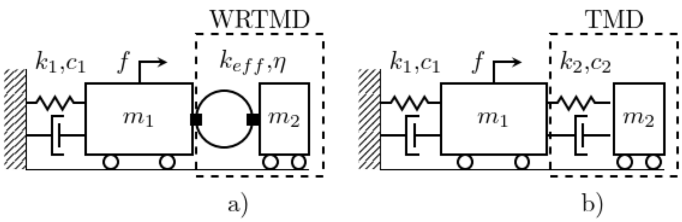

Figure 4. Illustration of the two degree of freedom system with the wire rope tuned mass damper (a) and with the linear tuned mass damper (b). The excitation is applied on the first degree of freedom (m_1). In the study, the response of both m_1 and m_2 are monitored.

System models

This section presents the systems used to investigate the performance of the wire rope tuned mass damper. Three systems were selected, one with two degrees of freedom, and two with four degrees of freedom. In all of these systems, one degree of freedom is used for the tuned mass damper. The systems are illustrated in Figure 4 and Figure 5, and the parameters are listed in Table 1 and Table 2. Two variations of the four DOF model (Case A and Case B) are used, where the stiffness and damping values are altered. The TMD is the same in both cases, to study the effect of TMD mistuning.

This study considers only forcing with constant amplitude regardless of the excitation frequency. To study the effect of nonlinearity, it is necessary to consider multiple excitation amplitudes. The excitation forces range between 100 N to 500 N, which is less than the static load due to the TMD mass. For the two degree of freedom system, the natural frequency of the primary mass is varied between 25 Hz and 32 Hz. The mass ratio between the primary mass and the auxiliary mass is kept constant. In the four degree of freedom

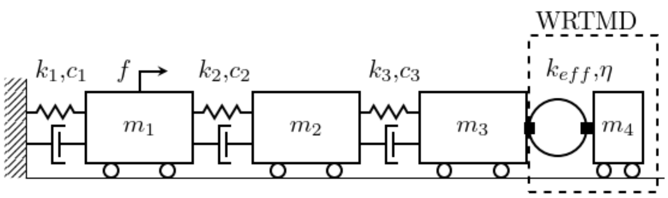

Figure 5. Illustration of the four degree of freedom system with the wire rope tuned mass damper. The excitation is applied on the first node. The fourth degree of freedom (m_4) is the tuned mass damper. It is not present in the undamped case. In the study, the response of m_3 is monitored.

Table 1. Model parameters for the two degree of freedom system illustrated in Figure 4. The mass ratio between the TMD and the system is 0.2. The wire rope TMD has 12 wire rope springs.

System ω_n (Hz)	m_1 (kg)	k_1 ($\mathrm{MN\,m^{-1}}$)	c_1 ($\mathrm{kN\,s\,m^{-1}}$)
25 Hz	480	11.84	3.02
32 Hz	480	19.40	3.86

Table 2. The system parameters for the four degree of freedom system illustrated in Figure 5. The fourth degree of freedom is the linear tuned mass damper which is not present in all of the cases. The linear tuned mass damper has been tuned for the Case A system which has lower stiffness values. The mass ratio between the TMD and the system is 0.11. The wire rope TMD has 4 wire rope springs.

Parameter	**dof 1**	**dof 2**	**dof 3**	**dof 4**
Mass (kg)	94	111	102	32
Stiffness in Case A ($\mathrm{MN\,m^{-1}}$)	3.67	3.53	3.60	0.285
Stiffness in Case B ($\mathrm{MN\,m^{-1}}$)	8.77	8.43	8.60	0.285
Viscous damping in Case A ($\mathrm{N\,s\,m^{-1}}$)	600	600	600	603
Viscous damping in Case B ($\mathrm{N\,s\,m^{-1}}$)	600	600	600	603

model, the excitation force is 190 N.

The performance of the wire rope tuned mass damper is compared to a linear tuned mass damper with similar mass ratio. The wire rope tuned mass damper consists of twelve WRSs placed in parallel. The values used for the WRS are given in Table 3. The amplitude dependent tuning frequency of the wire rope tuned mass damper is calculated using Equation 10 and is shown in Figure 6. Because the wire rope spring model has been identified for a certain preload mass level, the auxiliary mass is always equal to the mass used in the identification tests.

Results and discussion

In this section the simulation results for the systems under consideration are presented. The steady state response of the two investigated systems was simulated. The effect of linear and wire rope tuned mass damper was compared to the undamped system. This section also highlights design aspects for a wire rope tuned mass damper applications.

Two degree of freedom model

The response of the two degree of freedom system was calculated with multiple excitation forces and two different primary mass natural frequencies. The resulting responses for the primary mass (m_1) and the auxiliary mass (m_2) are shown in Figure 7. The Figure show that the maximum response of m_1 is below 25 Hz (Figure 7 a) with the wire rope TMD, while the maximum response with linear TMD is at frequencies higher than 25 Hz.

Table 3. Model parameters for the Wire rope spring used in the study. Parameters with indices belong to loss energy model, while parameters without the indices belong to the stiffness model.

a_1 ($\mathrm{J\,m^{-3}}$)	b_1 ($\mathrm{J\,m^{-2}}$)	c_1 ($\mathrm{J\,m^{-1}}$)	b_2 ($\mathrm{J\,m^{-2}}$)	c_2 ($\mathrm{J\,m^{-1}}$)	x_a (m)	a ($\mathrm{N\,m^{-4}}$)	b ($\mathrm{N\,m^{-3}}$)	c ($\mathrm{N\,m^{-2}}$)	d ($\mathrm{N\,m^{-1}}$)
1.50e+5	0	0.3e-3	79.4	-0.01	0.2e-3	-8.86e+15	6.56e+12	-1.92e+9	3.56e+5

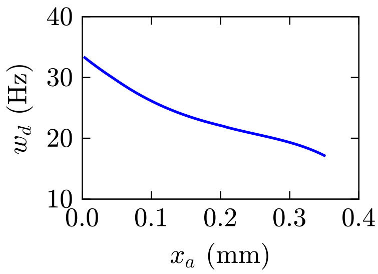

Figure 6. The tuning frequency of the wire rope tuned mass damper as a function of vibration amplitude. The tuning frequency is calculated with equation 10. The tuning frequency is calculated with only the auxiliary mass.

For the higher system natural frequency (Figure 7 b), the maximum peaks of both TMDs are at frequencies over the natural frequency of 32 Hz. WRTMD reduces the maximum amplitude more with higher load levels, while the linear TMD dampens the vibrations more with lower loads. The response of the linear systems is only amplified with increasing load.

The increasing excitation force amplitude has a significant effect on the response of the wire rope tuned mass damper. The Figure 7 shows a softening behavior, where the response peak shifts to a lower frequency as the excitation amplitude increases. The increase of loading from 100 N to 500 N shifts the response peaks by almost 3 Hz. Similar behavior has been observed in previous studies [3].

The results show that the WRTMD performs better as the excitation amplitude increases. At the lowest investigated load level the vibration amplitudes of both m_1 and m_2 are significantly higher with the WRTMD when compared to the linear TMD. The difference in the responses between the two TMDs is decreased as the load level increases. At the highest load level the WRTMD reduces the vibration of m_1 for the system with $\omega_n = 25\,\text{Hz}$, while for the system with $\omega_n = 32\,\text{Hz}$ the linear TMD still performs better. With higher frequencies the vibration amplitudes are also lower, which lead to less damping in the wire rope springs. It should also be noted that the maximum amplitude of the m_2 in the WRTMD is smaller when compared to the linear TMD at higher loads. This is due to the increased damping as the vibration amplitude of the wire rope spring increases.

Four degree of freedom model

The response of the third mass in Case A of the four degree of freedom system is shown in Figure 8 along with the mode shapes of the system without the TMD. The Figure shows that the wire rope TMD can reduce the response at the two lowest natural frequencies. The response of the third mode is slightly amplified. The linear tuned mass damper has a significant effect on the lowest natural frequency, and only small effect on the second mode.

The wide band damping capability was investigated by changing the system natural frequencies upwards while keeping the tuned mass dampers the same. The resulting response of Case B of the four degree of freedom model is shown in Figure 9 along with the mode shapes of the system without the TMD. The Figure shows that the linear tuned mass damper provides less damping for the first natural frequency, while the wire rope tuned mass damper still provides good vibration attenuation. The passive nonlinearity allows the damper to tune into multiple frequencies.

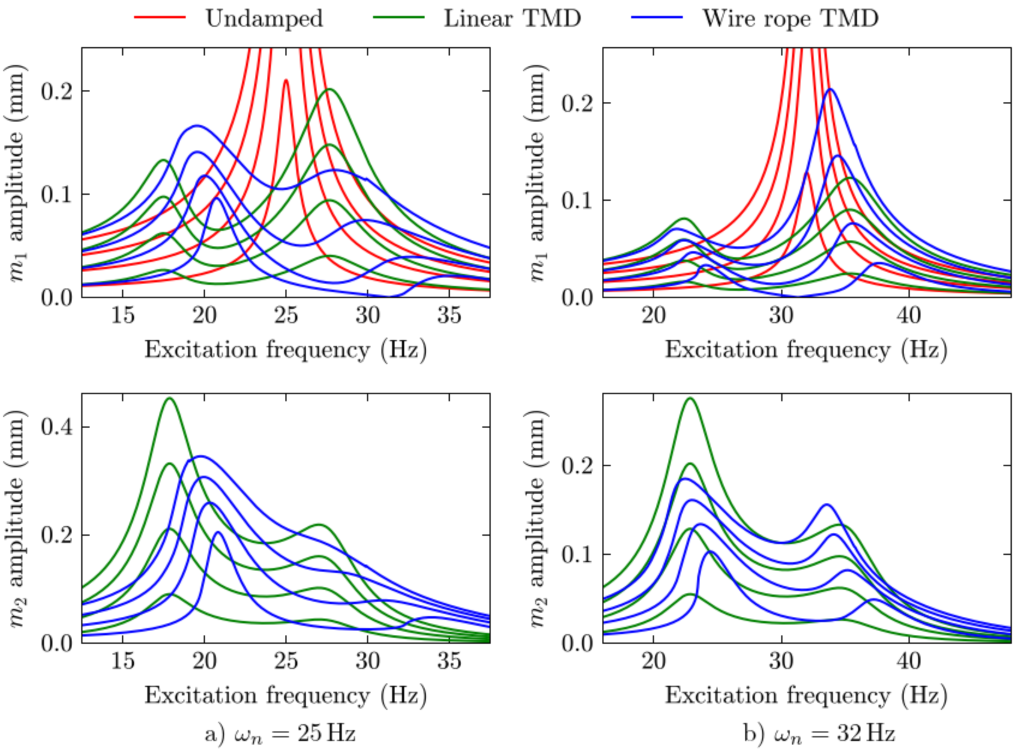

Figure 7. The response of the primary mass (m_1) and the auxiliary mass (m_2) in the two degree of freedom system (Figure 4). Two configurations of the system were analyzed, with difference being the stiffness of the of the primary mass spring (k_1). The different curves show the response of the system with linearly increasing load amplitude (from 100 N to 500 N). The resonance frequency of the linear systems stays constant, while the system with wire rope TMD shows a softening behavior. This means that the increasing force amplitude decreases the resonance frequency, changing the shape of the response.

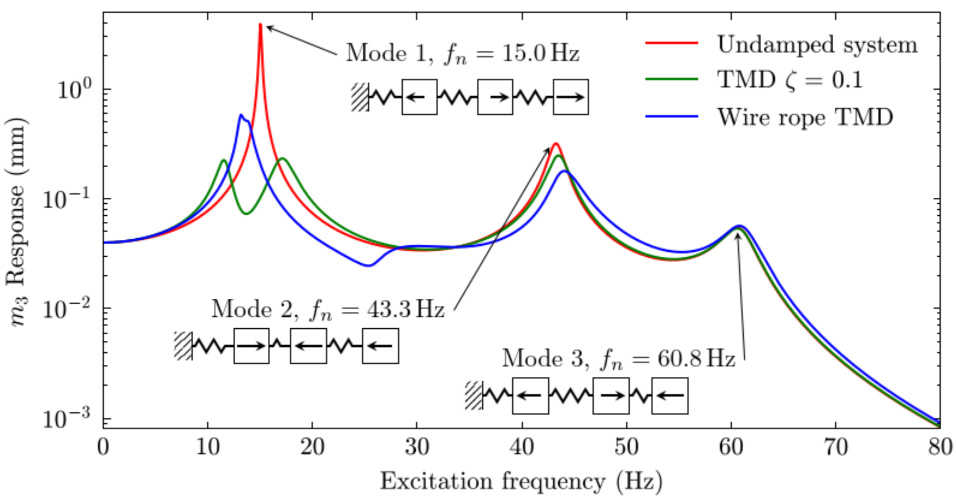

Figure 8. The response of the third mass in Case A of the four degree of freedom system (Figure 5, values in Table 2, force = 190 N). The linear tuned mass damper has been properly tuned to the first natural frequency. The wire rope tuned mass damper effectively dampens both the first and second peaks. The resonance peaks of the systems are highlighted with the arrows. Next to these arrows are the natural frequencies and mode shapes of the system without the mass damper.

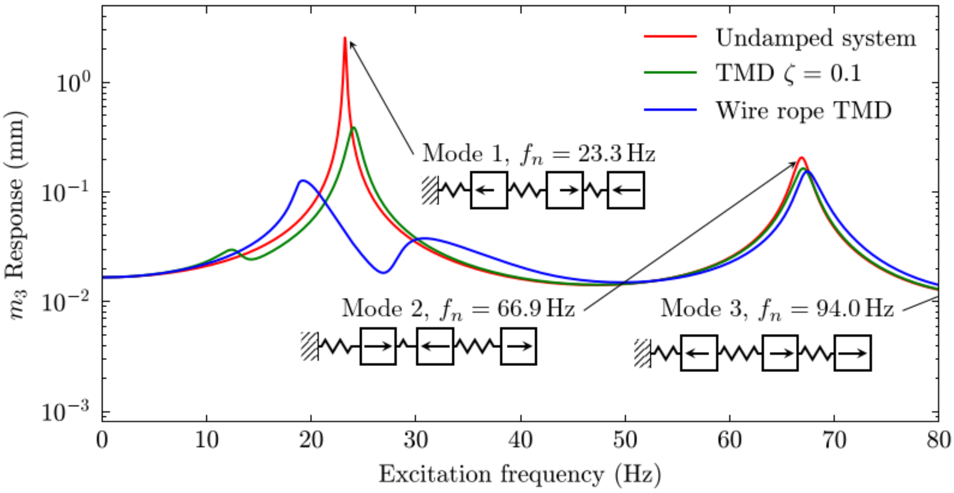

Figure 9. The response of the third mass in Case B of the four degree of freedom system (Figure 5, values in Table 2, force = 190 N), where the first natural frequency has been shifted from 15 Hz to 23 Hz. The second mode has shifted to 68 Hz and third mode to 120 Hz. The tuning frequency of the linear tuned mass damper is 15 Hz, showing limited damping performance. The wire rope tuned mass damper has remained unchanged from the system in Figure 8, showing that even though the resonance frequency has changed, the damping capability has not declined. The natural frequencies and mode shapes of a system without the tuned mass damper are presented next to the arrows. Third mode is outside of the excitation range.

Design process discussion

The design process for wire rope tuned mass damper is much more complicated than for a linear tuned mass damper. For the linear TMD equations have been developed to give the optimal stiffness and damping values for a certain mass ratio, which are easy to convert into real components. On the contrary, the amplitude dependent stiffness and energy loss curves are needed for each wire rope spring configuration. Currently there are no rules that tell how changing WRS parameters will affect the stiffness and damping. Therefore, the design needs to be done with a discrete set of identified WRS geometries and multiple design studies need to be carried out to find the optimal design. Optimal configuration for the system under consideration might not be available.

One of the main advantages of the wire rope tuned mass damper is its ability to dampen resonances on a wide frequency band. By comparing the Figure 8 (Case A) and 9 (Case B), it can be seen that the same wire rope tuned mass damper provides damping for both systems, while the linear tuned mass damper struggles with Case B. This indicates that the vibration suppression performance of the wire-rope spring TMD is to a certain degree more robust in comparison to the linear TMD for varying system natural frequencies and less susceptible to possible mistuning. This can be especially advantageous for systems where the natural frequencies change with time, such as a paper winders [14, 26].

Another important aspect of tuned mass damper design is the placement of the damper. It should be placed so that it is excited by the damped mode. Based on the mode shapes presented in Figures 8 and 9, the lowest mode has the highest amplitude in the third DOF. This is where the damper is located. This degree of freedom also has high amplitude on the two other modes. The location of the damper is always a compromise between the mathematical optimum and the constraints of the real world, as the damper cannot necessarily be placed the desired location. The presented model allows for efficient design study to find this optimum location.

There are several challenges when designing wire rope tuned mass dampers. Firstly, the mathematical model works only on the ranges where parameter identification has been made. Therefore amplitudes larger than those used in identification are not allowable. The mass of the WRTMD should not differ much from the preload mass used in the wire rope spring identification process, as it has some impact on the stiffness and energy loss curves [27]. Additionally, the load magnitude influences the damping capability of the WRTMD as shown in Figure 7. This means that the damper design might require modification if the excitation level changes. Finally, there is no published research on the long-term effects of vibration to the dynamic properties of wire rope springs. The wire surfaces wear due to friction, which over time changes the stiffness and damping of the wire rope springs before breaking them completely. This would pose an excellent topic for future research. Mechanical restrictior elements and preventive replacement of damaged wire rope springs can be used to mitigate the risk of total failure.

Most of the WRS related problems could be solved by identifying more WRS configurations or by researching methods to identify the parameters directly from the dimensions. Improved data availability can be used to create design rules on how the dimensions of the WRS affect the resulting stiffness and energy loss curves and therefore the performance of the tune mass damper. Until this can be solved, the experience of the designer plays a critical role on the performance.

Conclusion

This paper presented a simulation study on the use of wire rope springs based tuned mass damper which have not been previously considered in the literature. The study showed that the wire rope tuned mass damper can provide improved performance when compared to the linear tuned mass damper, especially if there are multiple natural frequencies that require damping or when the natural frequencies change. On the downside, the design process required more complicated. Further research is needed to facilitate effective design process.

Acknowledgments

The research was funded by Business Finland (Power Beyond, grant number 2534/31/2022).

References

[1] N.A. Alexander and F. Schilder. Exploring the performance of a nonlinear tuned mass damper *Journal of Sound and Vibration*, 319(1-2), 2009. https://dx.doi.org/10.1016/j.jsv.2008.05.018

[2] J.E. Brock. A note on the damped vibration absorber, *Journal of Applied Mechanics*, 13(4), 1946. https://dx.doi.org/10.1115/1.4009588

[3] N. Carpineto, W. Lacarbonara, F. Vestroni. Hysteretic tuned mass dampers for structural vibration mitigation, *Journal of Sound and Vibration*, 333(5), 2014. https://dx.doi.org/10.1016/j.jsv.2013.10.010

[4] G.F. Demetriades, M.C. Constantinou, A.M. Reinhorn. Study of wire rope systems for seismic protection of equipment in buildings, *Engineering Structures*, 15, 1993. https://dx.doi.org/10.1016/0141-0296(93)90036-4

[5] K. Dziedziech, A. Ghosh, J. Iwaniec, B. Basu, W, Staszewski, T. Uhl. Analysis of tuned liquid column damper nonlinearities, *Engineering Structures*, 171, 2018. https://dx.doi.org/10.1016/j.engstruct.2018.01.015

[6] H. Frahm. Device for damping vibrations of bodies, *US Patent*, US 989958 1909

[7] R.R. Gerges, B.J. Vickery. Design of tuned mass dampers incorporating wire rope springs: Part I: Dynamic representation of wire rope springs, *Engineering Structures*, 27(5), 2005. https://dx.doi.org/10.1016/j.engstruct.2004.12.015

[8] R.R. Gerges, B.J. Vickery. Design of tuned mass dampers incorporating wire rope springs: Part II: Simple design method, *Engineering Structures*, 27(5), 2005. https://dx.doi.org/10.1016/j.engstruct.2004.12.014

[9] J.P. Den Hartog. *Mechanical Vibrationsm*. McGraw-Hill, New York (1934).

[10] L. Huang, X.D. Yang. Dynamics of a novel 2-DOF coupled oscillators with geometry nonlinearity, *Nonlinear Dynamics*, 111(20), 2023. https://dx.doi.org/10.1007/s11071-023-08809-9

[11] J.A. Inaudi, J.M. Kelly. Mass damper using friction-dissipating devices, *Journal of Engineering Mechanics*, 121(1), 1995. https://dx.doi.org/10.1061/(ASCE)0733-9399(1995)121:1(142)

[12] V.Y. Janga, P.K. Gourishetty, B. Carboni, G. Quaranta, W. Lacarbonara. Hysteretic tuned mass damper with bumpers for seismic protection: Modeling, identification, and shaking table tests, *Journal of Sound and Vibration*, 597(A), 2025. https://dx.doi.org/10.1016/j.jsv.2024.118816

[13] C. Jolicoeur. Comparative Study of Two Semicontinuous Models for Wire Strand Analysis, *Journal of Engineering Mechanics*, 123(8), 1997. https://dx.doi.org/10.1061/(ASCE)0733-9399(1997)123:8(792)

[14] M. Jorkama. The Role of Analytical Winding Dynamics in Winder Design, *Tappi Journal*, 81(1), 1998.

[15] J .Keinänen, K. Vehviläinen. Self-tuned mass damper and system comprising the same. *US Patent*, US 2016123422), 2016.

[16] H. Laalej, Z.Q. Lang, B. Sapinski, P. Martynowicz. MR damper based implementation of nonlinear damping for a pitch plane suspension system, *Smart Materials and Structures*, 218(4), 2012. https://dx.doi.org/10.1088/0964-1726/21/4/045006

[17] L. Li, P. Cui. Novel design approach of a nonlinear tuned mass damper with duffing stiffness, *Journal of Engineering Mechanics*, 143(4), 2017. https://dx.doi.org/http://dx.doi.org/10.1061/(ASCE)EM.1943-7889.0001229

[18] S. Liu, H. Li, F. Zhang, Z. Lu, S, Yang, P. Li. The optimum design of particle tuned mass damper for structural seismic control considering soil-structure interaction, *Journal of Vibration and Control*, 30(7-8), 2023. https://dx.doi.org/10.1177/10775463231164198

[19] Z. Lu, X. Chen, Y. Zhou. An equivalent method for optimization of particle tuned mass damper based on experimental parametric study, *Journal of Sound and Vibration*, 419, 2018. https://dx.doi.org/10.1016/j.jsv.2017.05.048

[20] M.S. Miah, E.N. Chatzi, V.K. Dertimanis, F. Weber. Nonlinear modeling of a rotational MR damper via an enhanced Bouc-Wen model, *Smart Materials and Structures*, 24, 2015. https://dx.doi.org/10.1088/0964-1726/24/10/105020

[21] S.K. Mishra, S, Gur, S, Chakraborty. An improved tuned mass damper (SMA-TMD) assisted by a shape memory alloy spring, *Smart Materials and Structures*, 22, 2013. https://dx.doi.org/10.1088/0964-1726/22/9/095016

[22] O. Papailiou. Bending of helically twisted cables under variable bending stiffness due to internal friction , tensile force and cable curvature, *ETH ZURICH*, D.Sc Thesis, 1995.

[23] A.Y. Pisal, R. Jangid. Dynamic response of structure with tuned mass friction damper, *International Journal of Advanced Structural Engineering*, 8, 2016. https://dx.doi.org/10.1007/s40091-016-0136-7

[24] K. Rajana, Z. Wang, A. Giaralis. Optimal design and assessment of tuned mass damper inerter with nonlinear viscous damper in seismically excited multi-storey buildings, *Bulletin of Earthquake Engineering*, 21(3), 2023. https://dx.doi.org/10.1007/s10518-022-01609-3

[25] F. Rüdinger. Tuned mass damper with nonlinear viscous damping, *Journal of Sound and Vibration*, 300(3-5), 2007. https://dx.doi.org/10.1016/j.jsv.2006.09.009

[26] S. Rytömaa, S. Laine, R. Viitala. Rotordynamic Investigation of Roll Bouncing Phenomenon in Two-Drum Winder. *Advances in Mechanism and Machine Science. IFToMM WC 2023. Mechanisms and Machine Science*, 147, 2023. https://dx.doi.org/10.1007/978-3-031-45705-0_86

[27] S. Rytömaa, O. Malmi, S. Laine, J. Keinänen, R. Viitala. Wire rope isolator identification and dynamic modeling for small amplitude vibrations, *Engineering Structures*, 318, 2024. https://dx.doi.org/10.1016/j.engstruct.2024.118721

[28] K.M. Shum. Tuned vibration absorbers with nonlinear viscous damping for damped structures under random load, *Journal of Sound and Vibration*, 346, 2015. https://dx.doi.org/10.1016/j.jsv.2015.02.003

[29] C. Sun, S. Nagarajaiah, A. Dick. Experimental investigation of vibration attenuation using nonlinear tuned mass damper and pendulum tuned mass damper in parallel, *Nonlinear Dynamics*, 78, 2014. https://dx.doi.org/10.1007/s11071-014-1619-3

[30] M.L. Tinker, M.A. Cutchins. Damping phenomena in a wire rope vibration isolation system, *Journal of Sound and Vibration*, 157(8), 1992. https://dx.doi.org/10.1016/0022-460X(92)90564-E

Samuli Rytöamaa, Sampo Laine, Raine Viitala
Aalto University, Department of Energy and Mechanical Engineering
Puumiehenkuja 5, 02150 Espoo
samuli.rytomaa@aalto.fi